Supporting Information

for

Remarkable effect of π-skeleton conformation in finitely conjugated polymer semiconductors

Zhihui Chen,[ab] Weifeng Zhang,*[a] Yankai Zhou,[ab] Xuyang Wei,[ab] Chenyu Li,[ab] Liping Wang[c] and Gui Yu*[ab]

[a] *Beijing National Laboratory for Molecular Sciences, CAS Research/Education Center for Excellence in Molecular Sciences, Institute of Chemistry, Chinese Academy of Sciences, Beijing 100190, P. R. China*

[b] *School of Chemical Sciences, University of Chinese Academy of Sciences, Beijing 100049, P. R. China*

[c] *School of Materials Science and Engineering, University of Science and Technology Beijing, Beijing 100083, P. R. China*

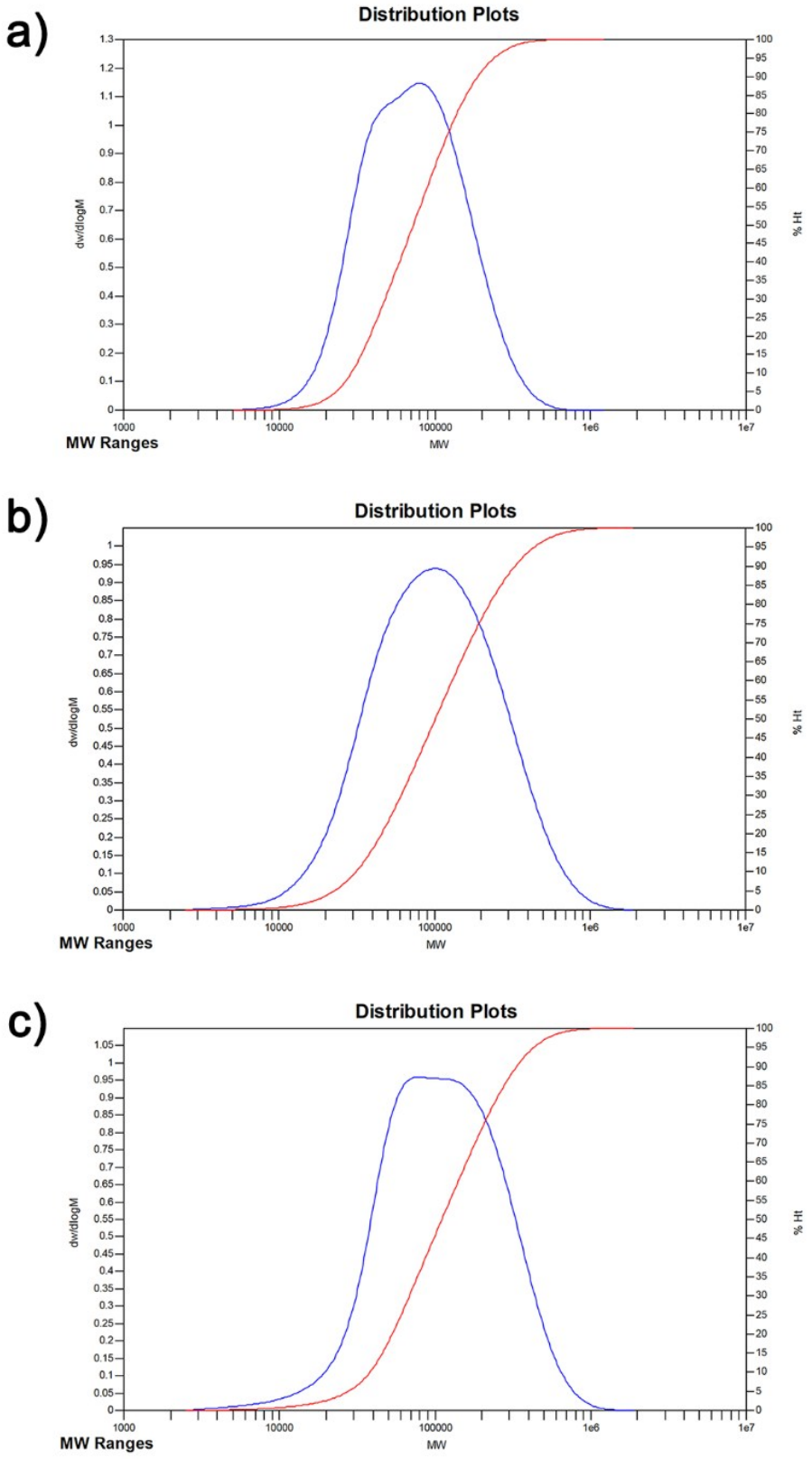

Fig. S1 High-temperature gel permeation chromatography (HT-GPC) plots of the TFE-containing finitely conjugated polymers, (a) **PNBDO-T**, (b) **PNBDO-BiT**, and (c) **PNBDO-TriT**.

Table S1 Molecular weight and distribution of the TFE-containing finitely conjugated polymers[a)]

	M_p	M_n	M_v	M_w	M_z	M_z+1	$Đ$
PNBDO-T	80484	55914	86495	93335	150074	219256	1.6693
PNBDO-BiT	102766	65227	131983	147906	291618	475939	2.2676
PNBDO-TriT	78540	72664	139389	153873	276069	420239	2.1176

[a)] GPC versus polystyrene standards in 1,2,4-trichlorobenzene at 150 °C.

Table S2 UPS spectra parameters of polymer thin films[a)]

polymer	E_{cutoff} (eV)	$E_{H,\,onset}$ (eV)	IP (eV)
PNBDO-T	16.93	1.60	5.89
PNBDO-BiT	16.89	1.49	5.82
PNBDO-TriT	16.94	1.36	5.62

[a)] IP = $h\nu - (E_{cutoff} - E_{H,\,onset})$, $h\nu$ = 21.22 eV.

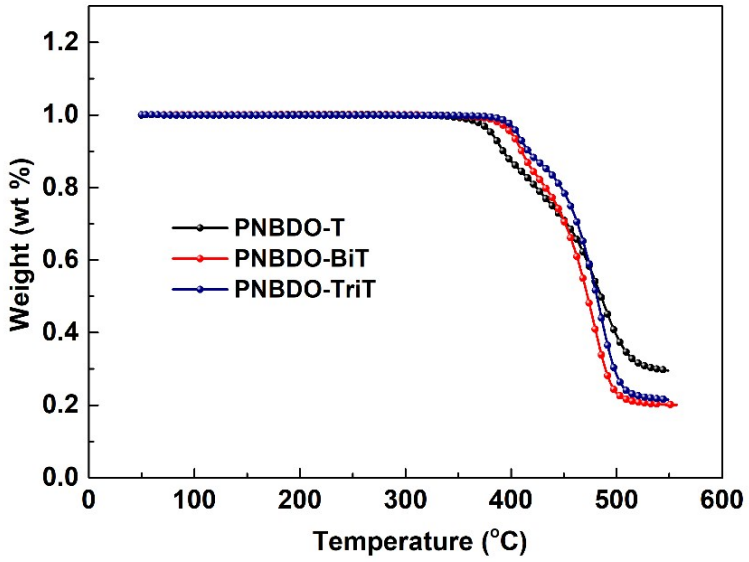

Fig. S2 TGA traces of the TFE-containing finitely conjugated polymers, **PNBDO-T**, **PNBDO-BiT**, and **PNBDO-TriT**.

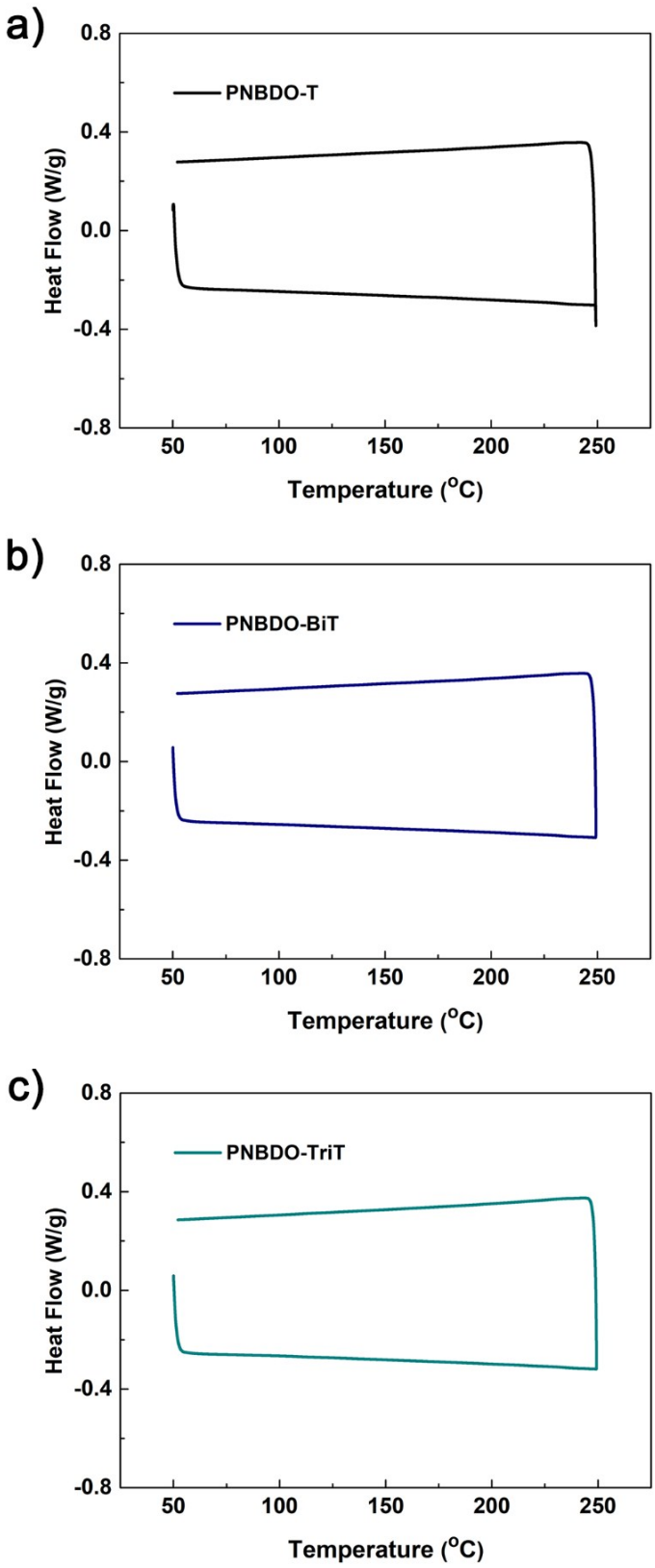

Fig. S3 DSC curves of the TFE-containing finitely conjugated polymers, (a) **PNBDO-T**, (b) **PNBDO-BiT**, and (c) **PNBDO-TriT**.

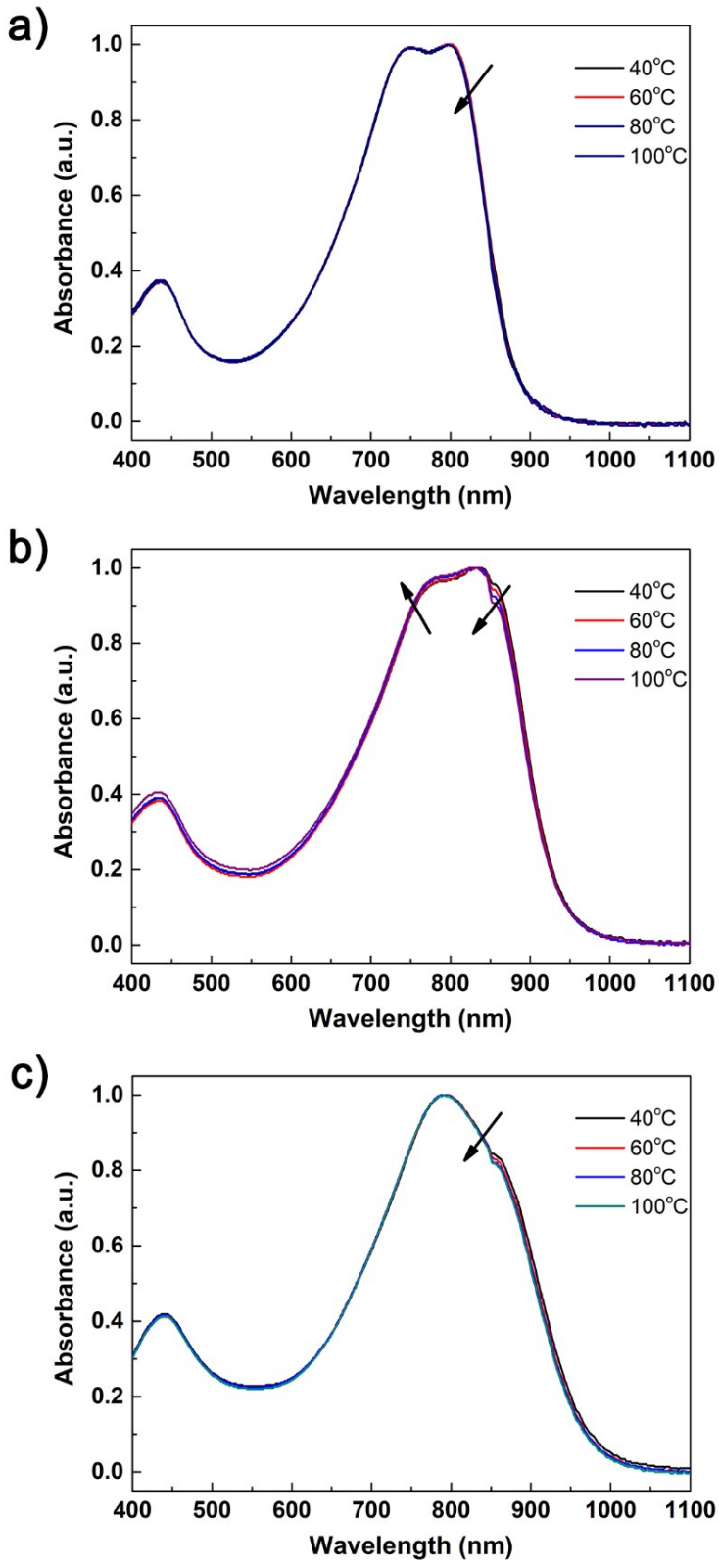

Fig. S4 Temperature-dependent absorption profiles of the TFE-containing finitely conjugated polymers, (a) **PNBDO-T**, (b) **PNBDO-BiT**, and (c) **PNBDO-TriT**, in dilute chlorobenzene solution.

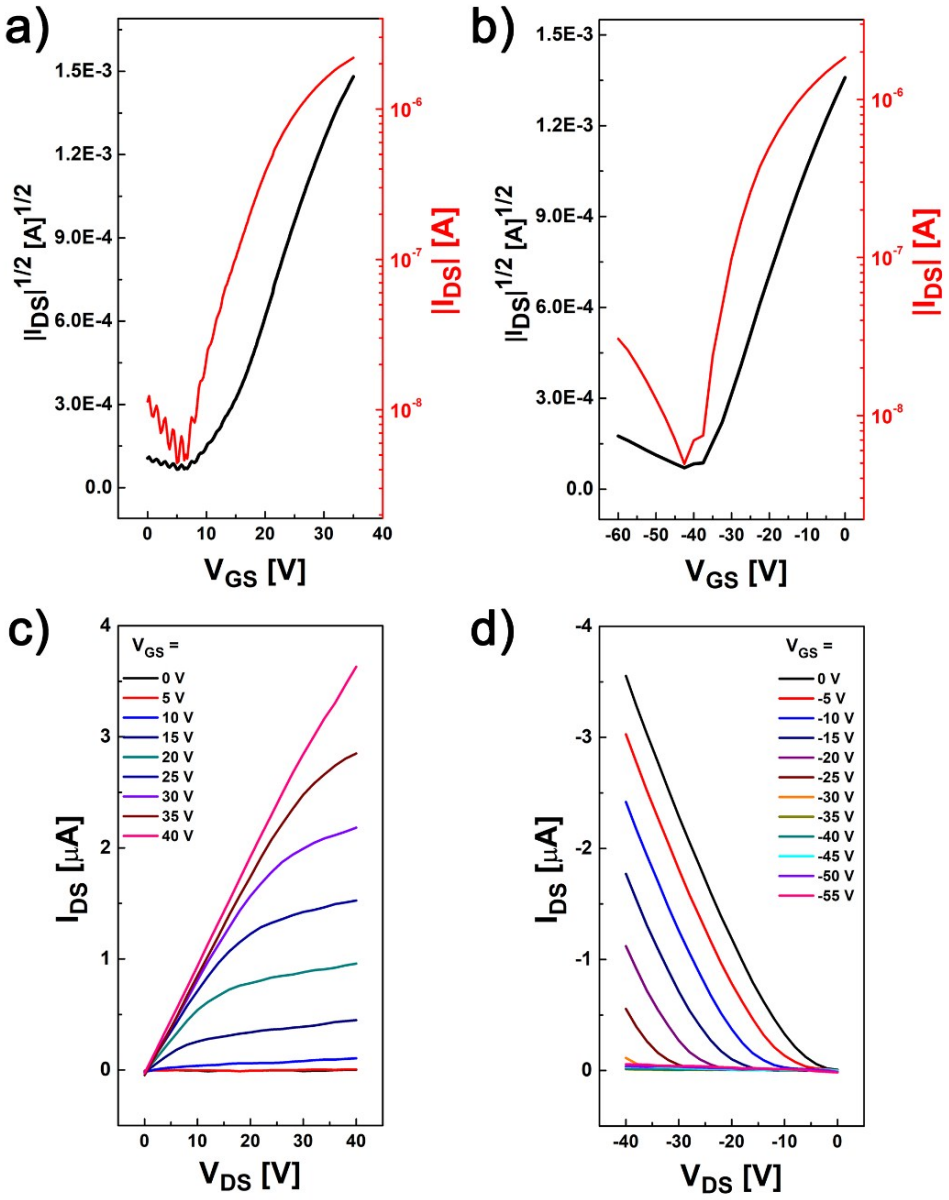

Fig. S5 Transfer characteristics (V_{DS} = −40 and 40V) and output characteristics of flexible FETs based on **PNBDO-T**.

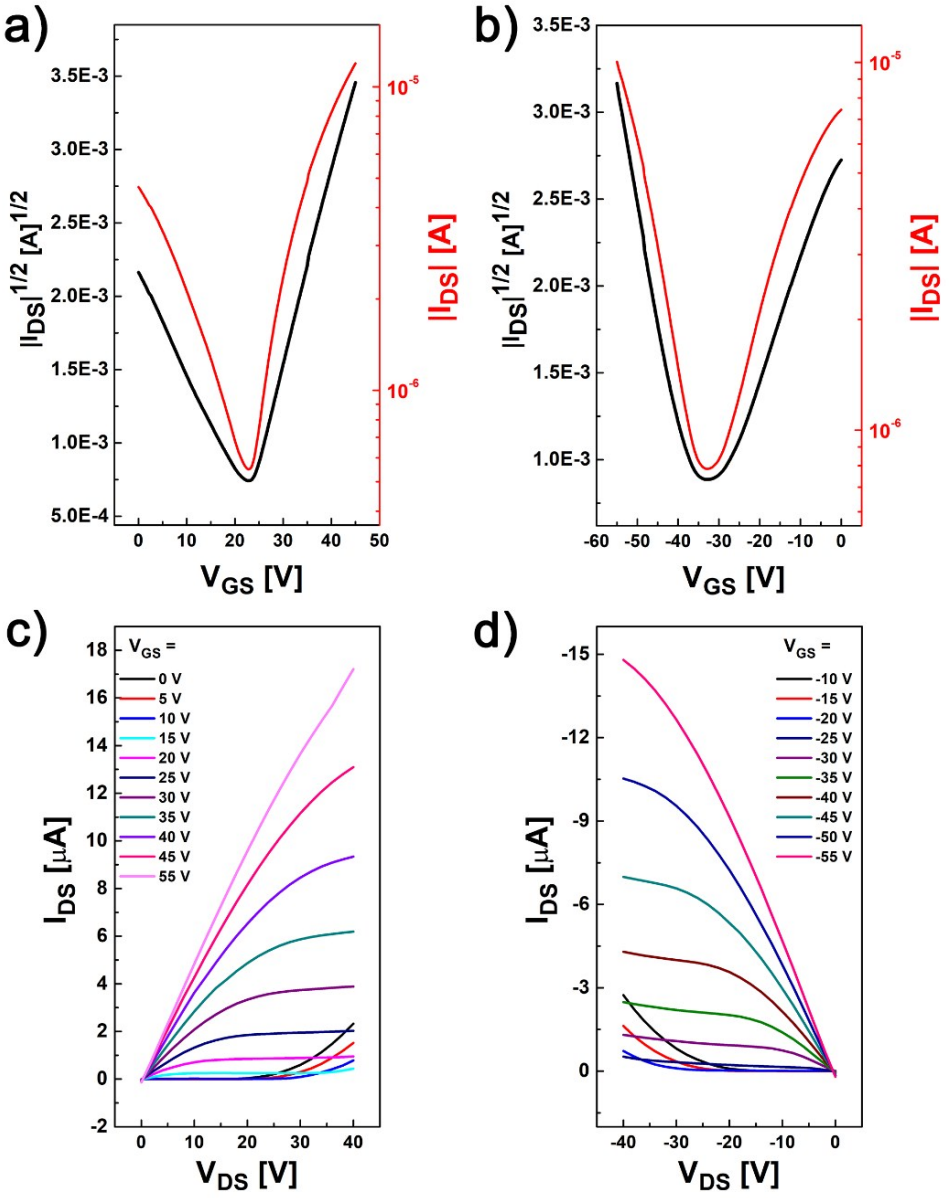

Fig. S6 Transfer characteristics (V_{DS} = −40 and 40V) and output characteristics of flexible FETs based on **PNBDO-TriT**.

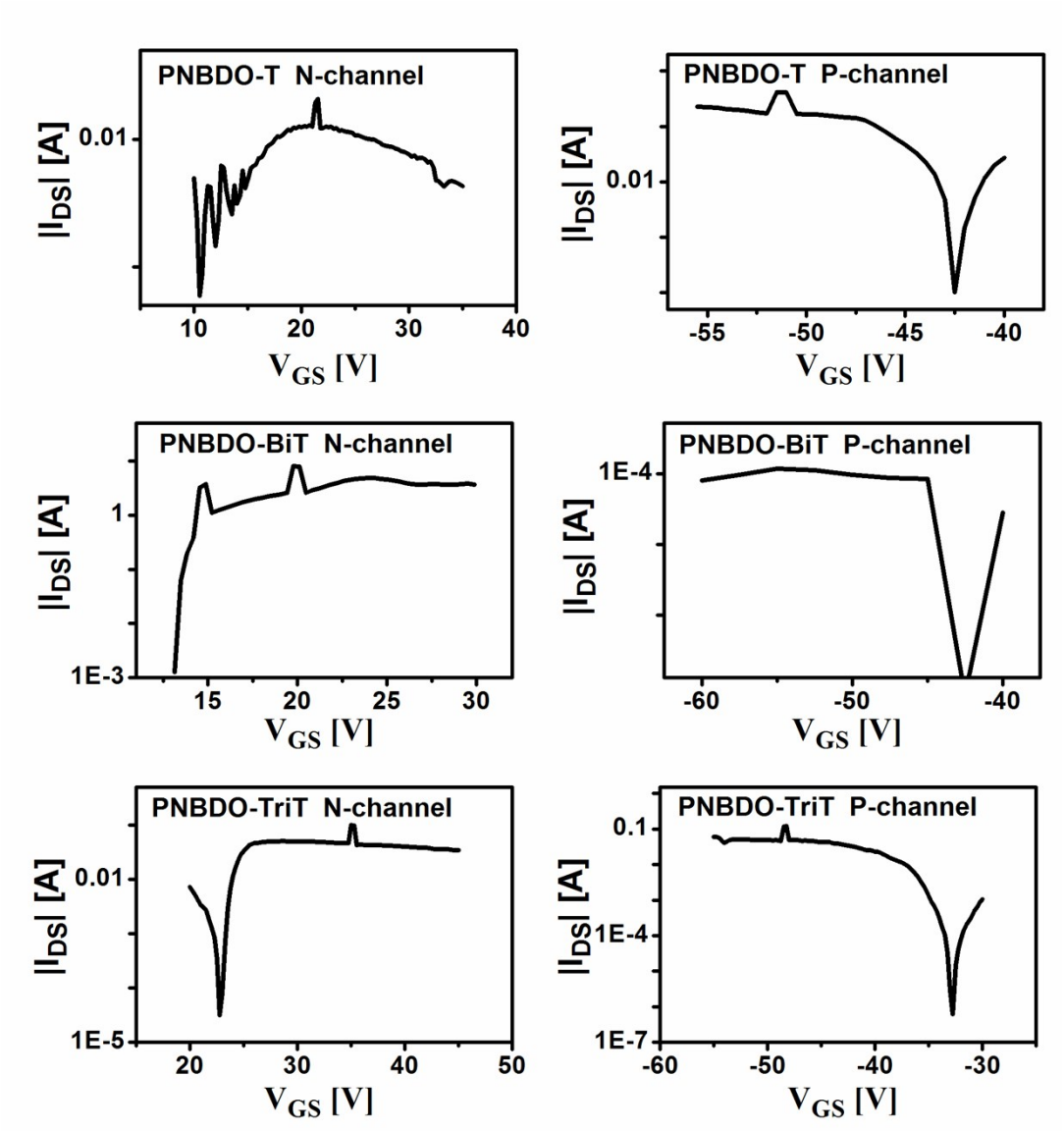

Fig. S7 Mobility versus gate voltage characteristics.

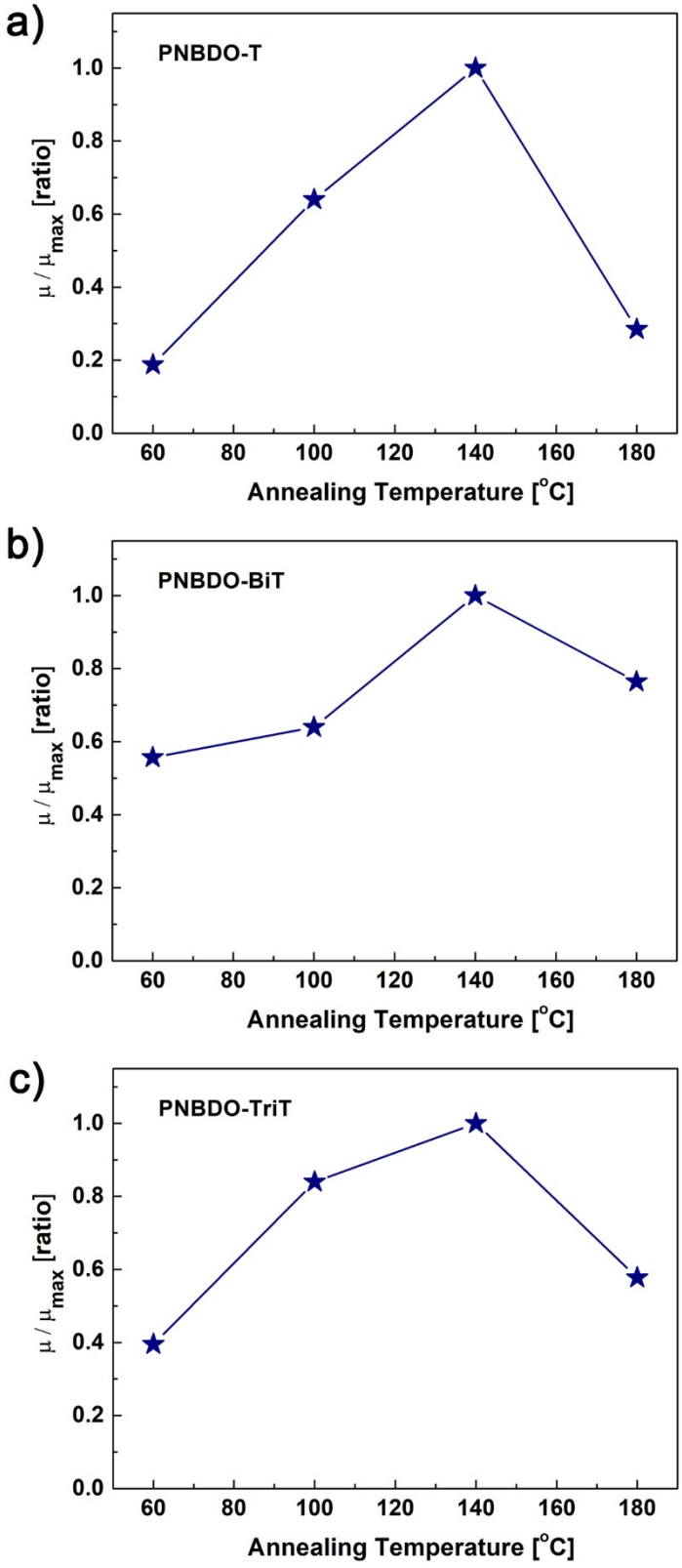

Fig. S8 Normalized annealing temperature-dependent electron mobilities of (a) **PNBDO-T**-, (b) **PNBDO-BiT**-, and (c) **PNBDO-TriT**-based FETs.

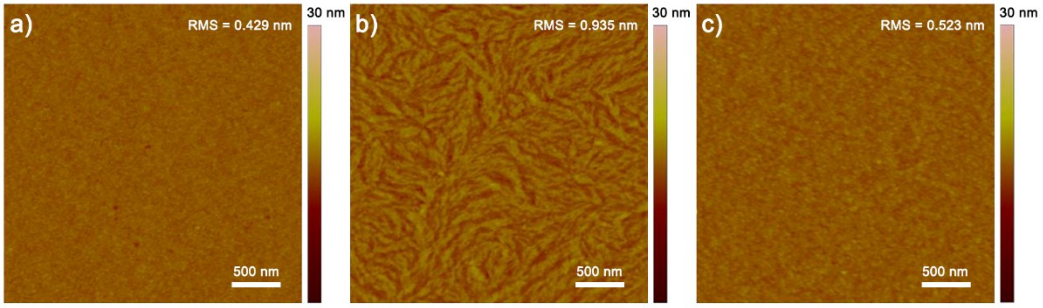

Fig. S9 AFM height images of the as-spun polymer thin films spin-coated on PET substrate, (a) **PNBDO-T**, (b) **PNBDO-BiT**, and (c) **PNBDO-TriT** (3 μm × 3 μm).

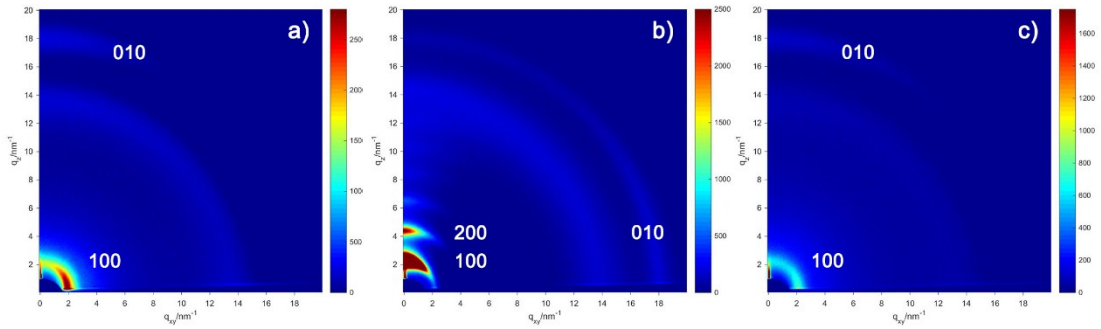

Fig. S10 2D-GIXRD diffraction pattern of the as-spun polymer thin films spin-coated on SiO_2/Si substrate, (a) **PNBDO-T**, (b) **PNBDO-BiT**, and (c) **PNBDO-TriT**.

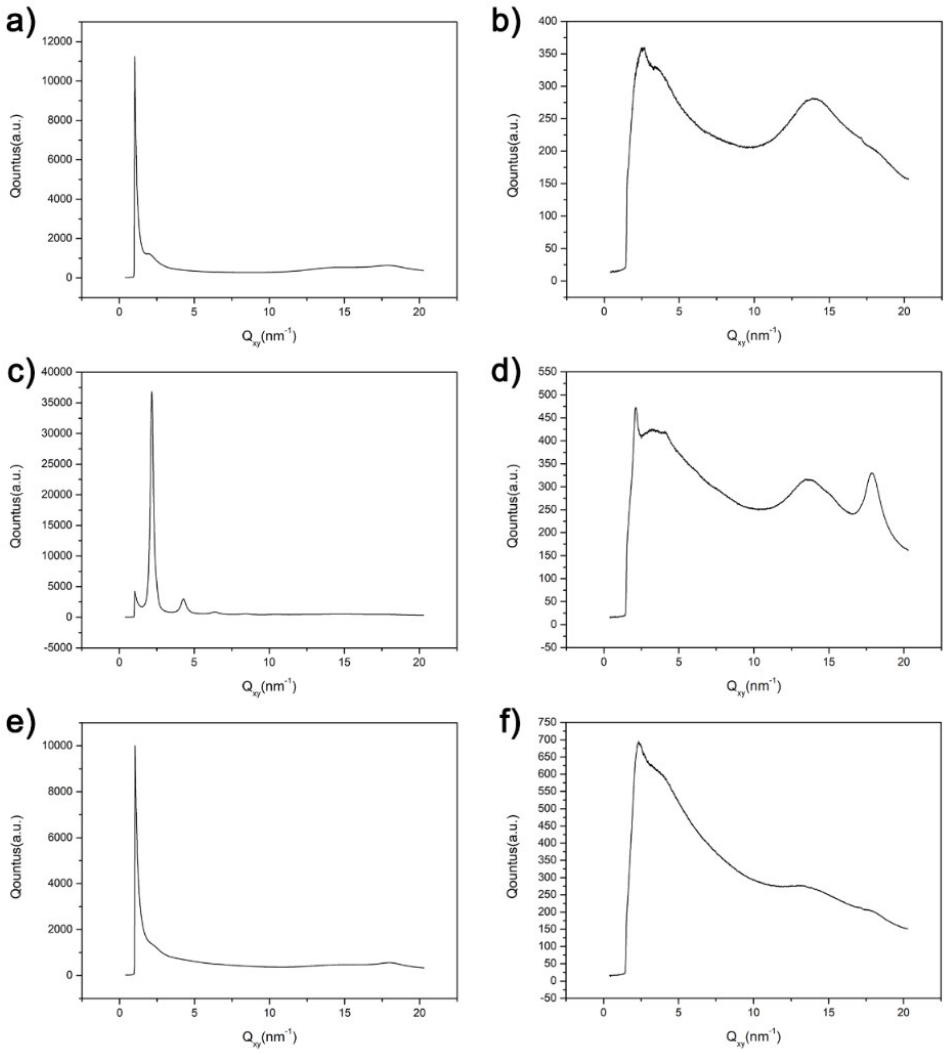

Fig. S11 1D-GIXRD diffraction pattern of the as-spun polymer thin films spin-coated on SiO_2/Si substrate: (a, c, and e) out-of-plane and (b, d, and f) in plane, (a, b) **PNBDO-T**, (c, d) **PNBDO-BiT**, and (e, f) **PNBDO-TriT**.

^{1}H and ^{13}C NMR spectra

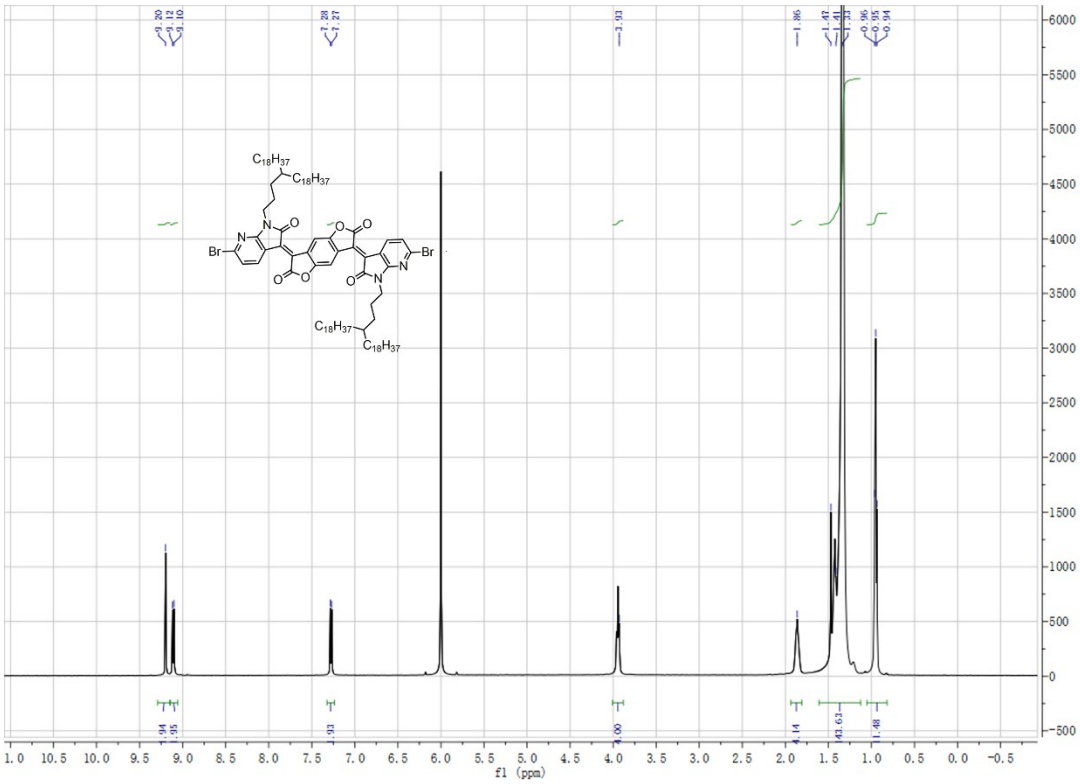

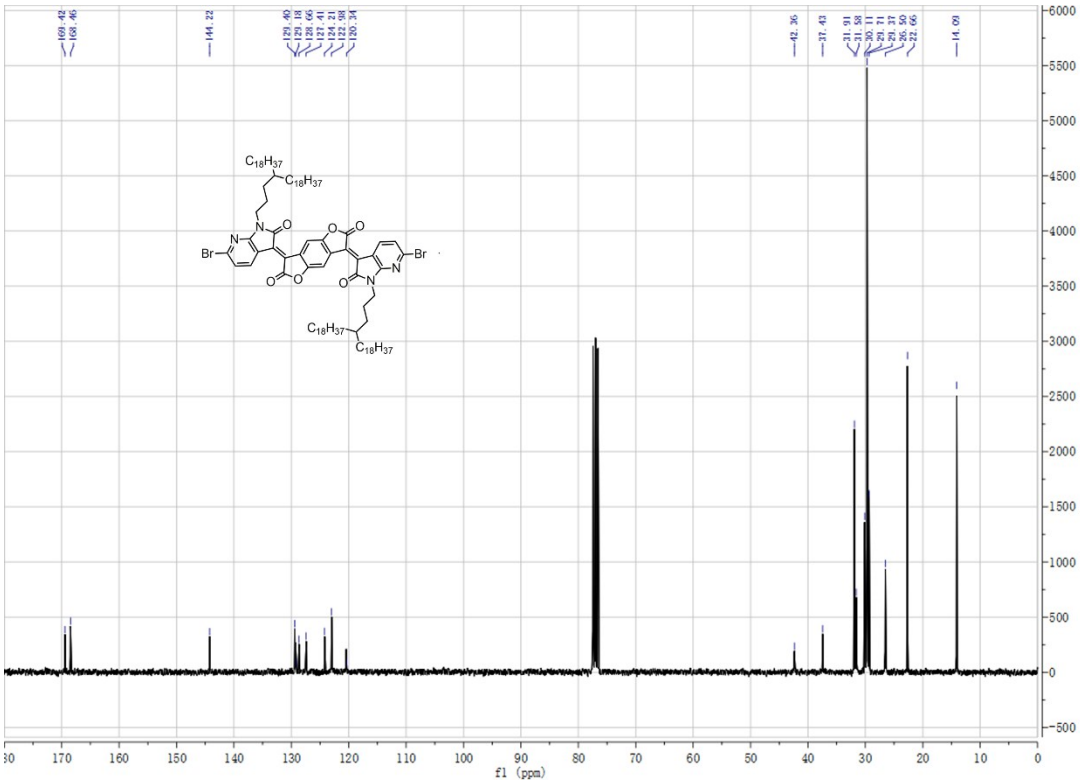

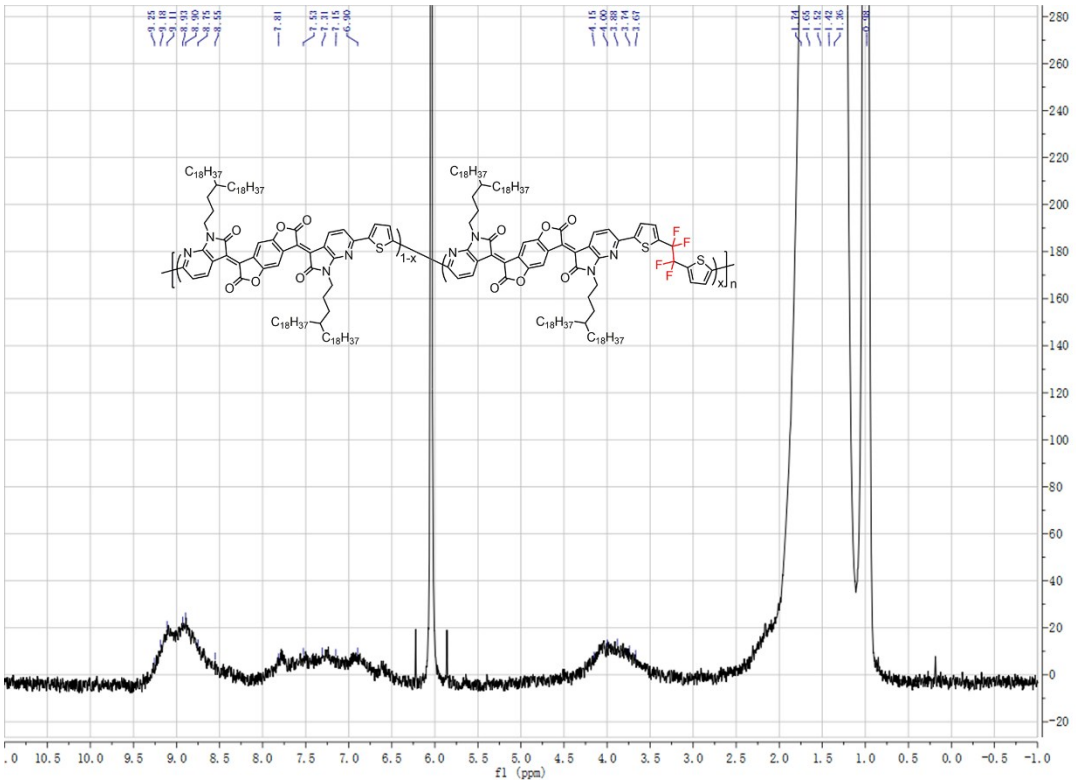
f1 (ppm)

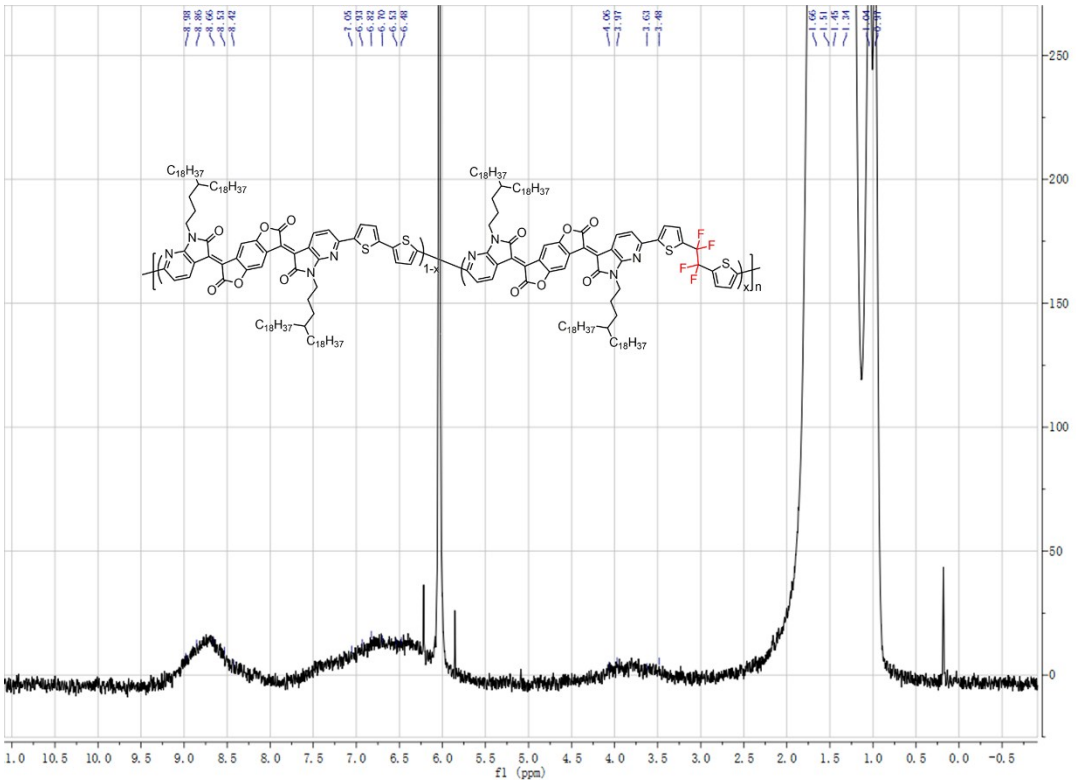
f1 (ppm)

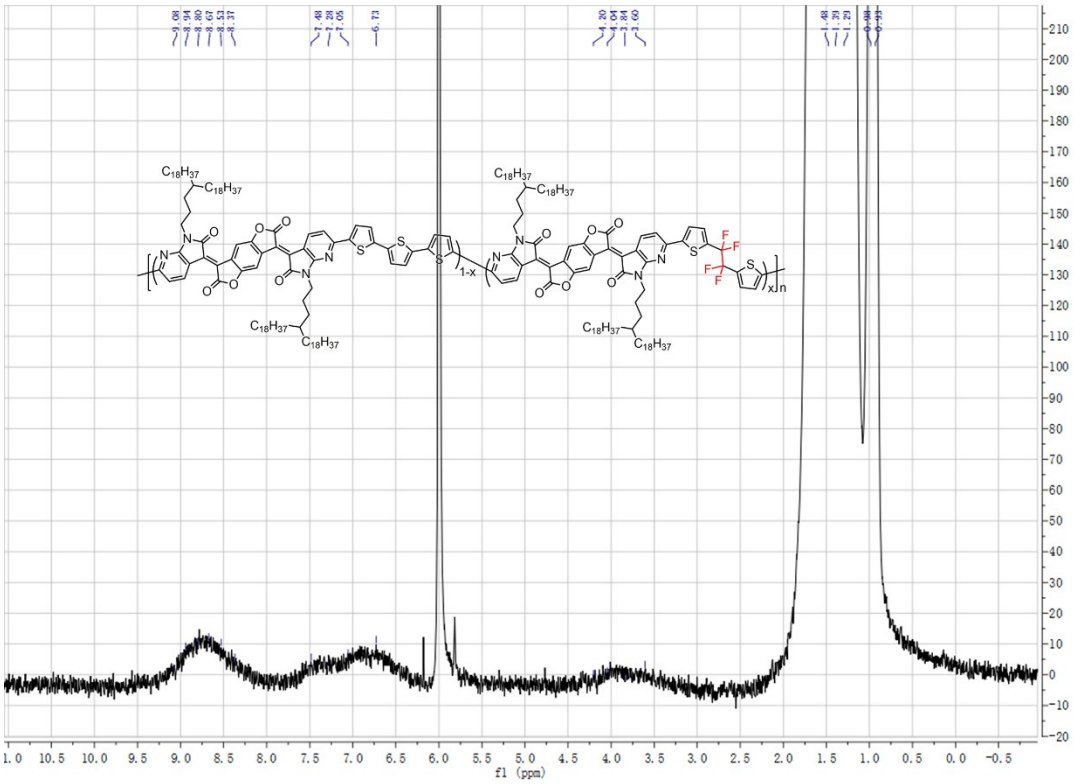
f1 (ppm)